INSTITUTE OF PHYSICS PUBLISHING SUPERCONDUCTOR SCIENCE AND TECHNOLOGY

Supercond. Sci. Technol. **16** (2003) 246–253 PII: S0953-2048(03)54598-5

The road to magnesium diboride thin films, Josephson junctions and SQUIDs

Alexander Brinkman, Dragana Mijatovic, Hans Hilgenkamp, Guus Rijnders, Ingrid Oomen, Dick Veldhuis, Frank Roesthuis, Horst Rogalla and Dave H A Blank

MESA+ Research Institute and Low Temperature Division, Applied Physics, University of Twente, PO Box 217, 7500 AE Enschede, The Netherlands

E-mail: d.h.a.blank@utwente.nl

Received 9 October 2002, in final form 14 October 2002
Published 3 January 2003
Online at stacks.iop.org/SUST/16/246

Abstract

The remarkably high critical temperature at which magnesium diboride (MgB_2) undergoes transition to the superconducting state, $T_c \approx 40$ K, has aroused great interest and has encouraged many groups to explore the properties and application potential of this novel superconductor. For many electronic applications and further basic studies, the availability of superconducting thin films is of great importance. Several groups have succeeded in fabricating superconducting MgB_2 films. An overview of the deposition techniques for MgB_2 thin film growth will be given, with a special focus on the *in situ* two-step process.

Although, meanwhile, many problems to obtain suitable films have been solved, such as oxygen impurities and magnesium volatility, the question of how single-phase epitaxial films can be grown still remains. The possibility of growing single-crystalline epitaxial films will be discussed from the deposition conditions' point of view as well as substrate choice. Necessary conditions are discussed and possible routes are reviewed.

The applicability of MgB_2 in superconducting electronic devices depends on the possibility of making well-controlled, i.e., reproducible and stable, Josephson junctions. The first attempts to make MgB_2–MgO–MgB_2 ramp-type junctions and SQUIDs from MgB_2 nanobridges are discussed.

(Some figures in this article are in colour only in the electronic version)

1. Introduction

The discovery of superconductivity in the intermetallic compound magnesium diboride (MgB_2) [1], with a remarkably high critical temperature at which this material undergoes transition to the superconducting state, $T_c \approx 40$ K, has aroused great interest and has encouraged many groups to explore the properties and application potential of this novel superconductor.

The initial reports were soon confirmed by Bud'ko *et al* [2], who described the occurrence of an isotope effect, hinting towards a phonon-mediated pairing-mechanism. The electronic structure of MgB_2 is now rather well understood and the superconductivity may be ascribed to the conventional electron–phonon mechanism [3–6]. The qualitative difference between the two-dimensional and the three-dimensional bands of the Fermi surface, in connection with the large disparity of the electron–phonon interaction (EPI) for the different Fermi-surface sheets suggested a multiband description of superconductivity [7–10]. Now, the interesting question arises, how the two-band superconductivity will be noticeable in the (temperature-dependent) electronic transport properties of MgB_2-based junctions [8, 11].

Apart from milestones like the realization of MgB_2 superconducting wires, as accomplished by Canfield *et al* [12], the investigations on the intergranular coupling [13, 14], and the determination of the coherence length of 50 Å [15] and energy gap values around 2.7 and 7.2 meV are important in the field of thin films and Josephson devices.

For many electronic applications and further basic studies, the availability of superconducting thin films is of great importance. The growth of thin films, however, was not an easy task and a number of problems had to be overcome, especially in order to obtain smooth and single-phase material suitable for multilayer structures which is important for the application in superconducting electronics. It took some time before issues such as oxygen impurities, low vapour pressure of magnesium, hardness (and ablation by excimer laser) of boron were solved. Although, meanwhile, many problems to obtain suitable films have been solved and several groups have actually succeeded in fabricating superconducting MgB_2 films, there is still the question how single-phase epitaxial films can be grown.

After an overview of the deposition techniques used to obtain thin films of MgB_2, the possibility of growing single-crystalline epitaxial films will be discussed, from the deposition conditions' point of view as well as substrate choice. The applicability of MgB_2 in superconducting electronic devices depends on the possibility of fabricating well controlled, i.e., reproducible and stable, Josephson junctions and vias. The first attempts to make junctions and superconducting quantum interference devices (SQUIDs) will be discussed and, finally, a prospect for MgB_2 thin films will be given.

2. Thin film deposition

The two main complicating factors for the fabrication of superconducting MgB_2 films are the high vapour pressure of magnesium and the high sensitivity of magnesium to oxidation, requiring very low oxygen partial pressures in the deposition system. Depending on the deposition technique, several options have been suggested to compensate for the possible loss of Mg in the deposition process. Roughly speaking, there are five different approaches that led to successful deposition:

1. *ex situ* post-anneal of boron films in magnesium overpressure [16–18];
2. *ex situ* post-anneal of Mg–B films in magnesium overpressure [19];
3. *in situ* post-anneal of Mg–B films, see figure 1 [20–24];
4. *in situ* post-anneal of Mg–B multilayers, see figure 1 [23, 25];
5. *in situ* (sputtering, MBE, CVD) deposition with high Mg flux [26–29].

In approach 1, a similar method has been used as in the wire technique, where magnesium is diffused into a boron wire at high temperature and high magnesium pressure [12]. A boron layer is deposited with MBE or pulsed laser deposition (PLD) at elevated temperatures. The deposition rate of boron is very low (∼0.1 Å/pulse at laser fluence of 8 J cm^{-2}). Subsequently, the film is annealed in a high-pressure cell with an Mg pellet at 900–950 °C for 1 h. The obtained T_c are comparable with bulk values, namely, ∼39 K. In principle, these films are suitable for theoretical studies, and transmission lines and filters. The surface roughness, however, is too large to use these films in multilayer configurations. During the diffusion of the Mg into the boron film, large grains and outgrowths occur. This morphology and the large surface

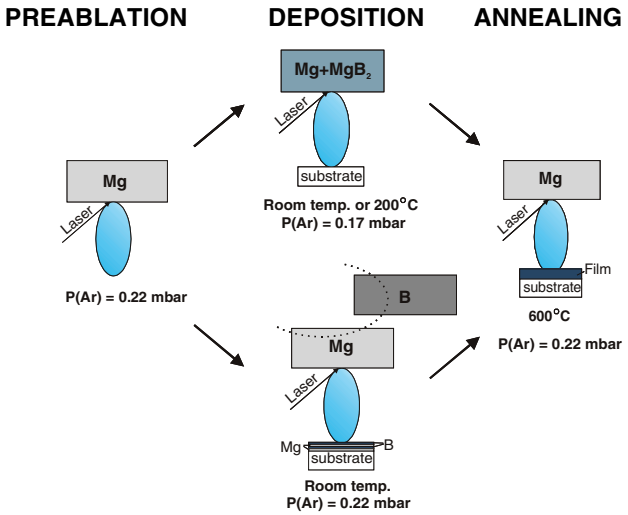

Figure 1. Schematic view of two different routes to deposit MgB_2 in the two-step *in situ* method. This method includes pre-ablation of magnesium to getter the oxygen and post-annealing to form the right phase.

roughness are clearly illustrated by the SEM pictures in [30]. In approach 2, the starting film is made by PLD or sputter deposition using a composite target. The obtained film, often made at room temperature, already has some magnesium (and probably also MgB_2) in the film composition. These films are annealed similar to the films discussed earlier and resulted in T_c of ∼35 K. The somewhat suppressed T_c may occur from impurities originating from the composite target. The surface quality reported is often better than the films made with the first approach. Approach 3, known as the two-step *in situ* deposition process, see figure 1, is the one most used up till now and will be discussed in more detail in the next paragraph. The obtained T_c are suppressed (∼30–34 K) but the surface roughness is much better than the post-annealed films. Approach 4, see figure 1, looks very promising but only a few attempts have been reported till now. The mean advantage is the 'separation' between the deposition of boron and magnesium, which makes it easier to avoid impurities. The ultimate procedure in this approach would be an atomic layer-by-layer deposition. Approach 5, deposition without any anneal step, has been reported lately. Although many groups have tried to deposit with MBE-like techniques, Ueda and Naito [27] were the first who succeeded, and this has been confirmed by Jo *et al* [28]. The success of their approach is the combination of depositing at lower temperatures (300 °C) at low background pressure and a very high magnesium flux. In the following, approaches 3 and 4 will be discussed, followed by the promising approach 5. Finally, in this thin film section, the requirements to gain single-phase epitaxial films will be discussed.

2.1. Two-step in situ deposition

To obtain good quality films, as far as reasonable T_c and surface roughness are concerned, the so-called two-step *in situ* method is most used so far. Using PLD, targets composed of MgB_2 powder enriched with Mg have been used to overcome the loss of magnesium. For example, targets were prepared from a mixture of 50 vol% Mg powder and 50 vol% MgB_2 powder.

These powders were carefully mixed and uniaxially pressed in the form of a pellet. Next, the pellets were sintered in a nitrogen flow for 3 h at 640 °C and subsequently for 10 h at 500 °C followed by a cool down to room temperature for about an hour. The obtained targets are very dense due to the melting of magnesium during target fabrication. The melting is very advantageous since only the surface will oxidize, which can be removed during pre-ablation.

During the experiments it was noticed that the plasma-plume invoked by the laser ablation process mostly showed a green colour, which is also typically observed in the growth of MgO. For the growth of elemental Mg, a blue plasma is to be expected. This suggested that the Mg was likely to oxidize during the deposition process, explaining the absence of superconductivity in the films. The colour of the plasma is dependent on the target material and background pressure during deposition, and varies in time too [20]. The time variation happens because of the role of Mg as a getter of the oxygen present. Amoruso *et al* [31] studied the dynamics of the plasma generated by pulsed-laser irradiation of a MgB_2 target, both in vacuum and at different Ar buffer gas pressures, by optical emission spectroscopy. Their analysis of the time-resolved emission of selected species shows that the Ar background gas strongly influences the plasma dynamics. Above a certain pressure, the plasma propagation into Ar leads to the formation of blast waves causing both an increase of the fraction of excited Mg atoms and a simultaneous reduction of their kinetic flux energy. This was also accomplished by a change in colour of the plasma, indicating the importance of this parameter.

The optimal Ar pressures to obtain the desired blue plasma will be dependent on the system used. In our case we found an optimal Ar pressure of 0.2 mbar with a KrF-laser energy $E = 500$ mJ. Using a laser spot size of approximately 8 mm^2 on the target, we obtained an energy density of about 4 J cm^{-2} at the target.

A typical deposition run is as follows (see also figure 1): first a Mg target is pre-ablated for 2 min at 10 Hz. This is done to reduce the oxygen background pressure in the chamber by the gettering action of the Mg. Before the pre-ablation, the chamber was filled with 0.2 mbar of Ar, at an Ar flow rate of 20 ml min^{-1}. Subsequently, the target composed of the Mg–MgB_2 mixture was pre-ablated under the same conditions, first for 2 min at 3 Hz and then for 1 min at 10 Hz. For the actual deposition, the pressure in the chamber was adjusted to the optimal value of 0.17 mbar and the substrate was placed in front of the target at a distance of 4.5 cm (on-axis geometry). The films were deposited at a repetition rate of 10 Hz for 6 min, yielding an approximate layer thickness of 220 nm.

The deposition temperature is crucial to obtain superconducting films. In principle, one likes to grow the film at temperatures as high as 650 °C. However, this is not possible due to the evaporation of the magnesium. The deposition temperature has to be kept as low as 300–350 °C. Therefore, a high-temperature annealing step is needed to form the superconducting phase. In our case, the annealing procedure took place in a 0.2 mbar Ar atmosphere using an Ar flow of 20 ml min^{-1} and consisted of a rapid increase (in 4 min) to $T_{ann} = 600$ °C followed by a quick cool down in the same Ar atmosphere to 500 °C, where it is kept for 60 min. Afterwards, it is cooled to room temperature at a rate of 50 °C per min. The total annealing procedure has to be kept short to avoid Mg evaporating out of the film. During the anneal procedure, several processes take place: MgB_2 phase formation, evaporation of magnesium, nucleation and growth of crystallites.

The T_c of the film is suppressed ($T_c \sim 30$ K), whereas the critical current density at 20 K exceeds 10^6 A cm^{-2}. The reason for this suppression is under debate since the first publications on thin films appeared. Three clear statements can be made: all films have oxygen (and carbon) impurities through oxidation of Mg and B, only very small grains are obtained and only very small intensity peaks are obtained applying x-ray diffraction. The results are almost independent of the substrates used (mostly MgO, sapphire, $SrTiO_3$).

The highest T_c reported, using this method, is obtained by Xi *et al* [32]. They refer to a T_c of 34 K. The MgB_2 films were deposited on (0001) Al_2O_3 substrates from targets prepared by pressing Mg powder with MgB_2 powder without sintering. The Mg:MgB_2 molar ratio was varied between 4:1 and 2:1. The films were deposited at 250–300 °C in an Ar atmosphere (5N gas purity). The energy density of the laser beam was 5 J cm^{-2}, with a repetition rate of 5 Hz. The deposited films were then annealed at 630 °C for 10 min. The atmosphere during deposition and annealing was 120 mTorr. After the *in situ* annealing, the films were cooled to room temperature in 20 Torr Ar. Also, they could not observe any XRD peaks originating from MgB_2, although ac-susceptibility measurements show a clear superconducting transition. The absence of XRD peaks in films made with this approach could indicate that the grain size of MgB_2 is extremely small, of the order of nanometres. This could also limit the superconducting properties of the films. A longer annealing time will improve the grain size, but simultaneously increase the evaporation of Mg and decomposition of MgB_2.

Mijatovic *et al* [25] showed results using multilayered films, as indicated by approach 4 and schematically drawn in figure 1. The multilayers were grown from magnesium and boron metal targets on MgO substrates. The multilayer is deposited at room temperature. The pre-ablation and annealing procedure were the same as for the above-described deposition from the Mg enriched MgB_2 target. The highest $T_{c;\,zero}$ of ∼30 K was obtained by depositing the magnesium metal in an Ar pressure of 0.22 mbar for 1 min at 10 Hz and, subsequently, boron metal for 3 min at 25 Hz. This is repeated 10 times, leading to a film thickness of 180 nm. Also, using this method, no XRD peaks of the MgB_2 reflections could be observed, indicating that the grain size is still small. Because of the fact that the two targets are metallic instead of a composite, it is likely that less oxygen is incorporated in the film. This could be the reason why the multilayer technique leads to higher T_c, even without an extra anneal step at 500 °C.

2.2. Are epitaxial films possible?

Although some applications of MgB_2 thin films do not require epitaxy, it is strongly desired in the case that one wants to make use of the exceptionally large I_cR_N product for tunnelling in the *a–b* direction [8] and the low-resistive behaviour in the normal state. Furthermore, the reproducibility and reliability

of all Josephson devices will rely on the degree of epitaxy and smoothness of the MgB_2 thin films, underlining the need for an epitaxial growth procedure.

In addition to the results obtained from approaches 3 and 4, the MBE results of Ueda and Naito (approach 5) show high T_c and indications of a MgB_2-XRD pattern. They succeeded in obtaining as-grown superconducting films in a limited growth temperature range of 150–320 °C. At such low temperatures, films are poorly crystallized but show a sharp superconducting transition (<1 K) of as high as 36 K. In their method, the use of a higher growth temperature to improve the crystallinity failed because the Mg in the films was almost completely lost. Ueda and Naito have grown films on various substrates ($SrTiO_3$ (001), sapphire-R, sapphire-C and Si (111)). The base pressure was as low as 10^{-9} Torr and pure metal sources using multiple electron beam evaporators were used [33]. The evaporation beam flux of each element was controlled by electron impact emission spectrometry (EIES) via feedback loops to electron guns. To avoid Mg loss, the flux ratio Mg:B was varied to 10 times as high as the nominal flux ratio. They obtained a growth rate of 2–3 Å s^{-1}, and deposited 100 nm thick films. The films made with deposition temperatures above 350 °C were Mg deficient (even if they apply a 10 times higher Mg rate). This limits the growth temperature significantly. The films deposited below 300 °C contained excess Mg, but that is not expected to influence the T_c of the film. However, in a multilayer configuration this may hamper the applicability of this method. In addition, XRD peaks originating from MgB_2 were not observed, except for the films deposited on sapphire-C substrates. These peaks, which can be attributed to MgB_2 (00*l*) peaks, are, however, very small. Reflective high energy diffraction (RHEED) showed spot patterns indicating a single-crystalline phase. The highest T_c were obtained using Si (111) and sapphire-C substrates. This may be due to the hexagonal structure of the substrate surface. After all, MgB_2 has a hexagonal crystal structure too, with hexagonal Mg and B planes stacked alternating along the *c*-axis, providing a better match. These results are confirmed by Jo *et al* [28] with the notice that they observed clear MgB_2 (00*l*) peaks with XRD.

An alternative method is suggested by Zeng *et al* [29] using a hybrid physical–chemical vapour deposition (HPCVD) process. In their process, the high Mg vapour pressure necessary to keep the MgB_2 phase thermodynamically stable is achieved by evaporating Mg, while the boron is deposited by CVD using B_2H_6 as the boron precursor gas. With this technique, films were grown epitaxially on (0001) sapphire and (0001) 4H–SiC substrates and show, besides a clear MgB_2 (00*l*) XRD pattern, a bulk-like T_c of 39 K, a J_c(4.2 K) of 1.2×10^7 A cm^{-2} in zero field and a H_{c_2} of 29.2 T in parallel magnetic field. They obtained smooth surfaces with a root-mean-square roughness of 2.5 nm for MgB_2 films on SiC.

In addition, Mijatovic *et al* [34] presented a method in which the boron is deposited by sputtering, and the magnesium flux can be (independently) tuned by pulsed laser ablation. The low heat conductivity of boron significantly influences the splashing during PLD of boron. Therefore, sputtering of boron seems to be a better way to deposit this material. On the other hand, with PLD of Mg one is able to vary the Mg flux by adjusting the laser frequency and shape of the plasma. The high Mg flux allows higher deposition temperature, which would lead to better crystallinity of the films.

2.3. Substrate choice

In epitaxial growth, the substrate choice is of utmost importance. Besides lattice matching, the reactivity between substrate and thin film and expansion coefficient also have to be taken into account. Because some of the applications of MgB_2 will be at high frequencies, the loss also has to be taken into account. In all cases, the reactivity of MgB_2 with the substrate material (or materials in multilayer circuits) is an important factor in determining the film fabrication and, thus, device characteristics. He *et al* [35] studied the reaction between MgB_2 and materials that are expected to be candidates for substrate or interlayer. They found that MgB_2 is inert for many common electronic and substrate materials at 600 °C. At these temperatures, a clear reaction was found for SiO_2 and Si. At 800 °C, MgB_2 was found to be inert with respect to ZrO_2, YSZ, MgO, TiN and AlN up to 700–800 °C. However, MgB_2 was highly reactive toward some of the most common substrate materials, i.e., Al_2O_3 and $SrTiO_3$, showing their limitations if high fabrication temperatures must be used during film deposition. Some reactions (by the shifting of MgB_2 diffraction peaks) were also observed using SiC. The latter could be the substrate of choice because of its perfect lattice match with MgB_2. As a buffer layer, Zhai *et al* [36] proposed TiB_2. They fabricated high quality layers on Si by PLD, which forms the right lattice match and a diffusion barrier for Si at high temperatures.

3. Towards superconducting electronic devices

Numerous groups have started investigating MgB_2 due to its great potential for large current and electronic applications. The reasons for the interest in using MgB_2 in superconducting electronics are manifold. The large charge carrier density and the corresponding low resistivity in the normal state [16], and the fact that grain boundaries in polycrystalline MgB_2 are strong links [13, 15] are important advantages as compared to the cuprate high temperature superconductors. In comparison with the conventional metallic superconductors, MgB_2 has the potential for higher operation speed due to its larger energy gap. Finally, the high transition temperature of MgB_2 facilitates cooling of superconducting electronic circuits by cryocoolers. Essential for the realization of superconducting electronics is the availability of high quality thin films and the technology to fabricate Josephson circuits based on these films.

3.1. Fabrication of MgB_2 Josephson junctions

Very soon after the first reports on thin films, the realization of various Josephson devices in MgB_2 was reported. These were based on, e.g., thin film nanobridges [37], localized ion damage [38, 39], point contacts [40, 41] and thin film heterostructures with one MgB_2 electrode [42–44]. To optimally exploit the beneficial properties of MgB_2 and to be able to tune the junction characteristics by choosing the barrier parameters, the challenging step was to realize MgB_2/artificial barrier/MgB_2 thin film junctions.

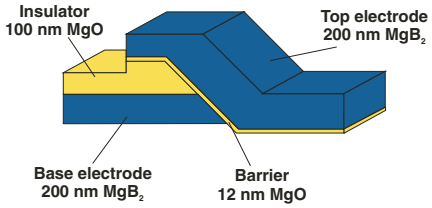

Figure 2. Schematic view of a ramp-type Josephson junctions. The ramp is defined by photolithography and, subsequently, ion milling. The barrier and top electrode are deposited without breaking the vacuum. Before depositing the barrier, a clean step has been carried out (so-called soft ion milling), see [47].

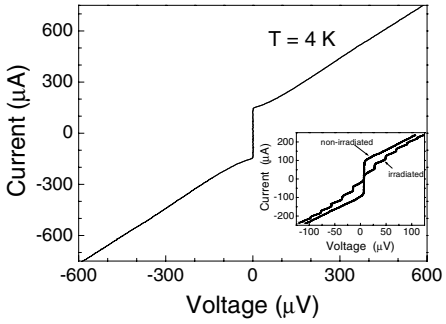

Figure 3. I–V characteristics of 7 μm wide junction measured at 4 K. The inset shows Shapiro steps that appear by irradiating the junction with 10.0 GHz microwave frequency (from [45]).

At present, some attempts have been made although no pure *tunnel* Josephson junctions have been reported yet. Mijatovic *et al* [45] reported the first fabrication and characteristics of multilayer Josephson junctions with two MgB_2 electrodes and a dielectric barrier material. The proper operation of these junctions is evidenced by a clear modulation of the supercurrent by applied magnetic fields and the occurrence of Shapiro steps under microwave irradiation. The junctions were prepared according to the ramp-type configuration [46] similar to the one that is used for the high temperature cuprate superconductors (figure 2). First, a bilayer of MgB_2 (200 nm) and MgO (100 nm) was deposited *in situ* by PLD on a MgO substrate. The MgB_2 film was prepared with a Mg-enriched MgB_2 target, using the procedure described above and published in more detail in [20]. After deposition, a bevelled edge (ramp) was defined by standard photolithography and argon ion beam etching under an angle of 45°.

Due to the difference in etching rate with the photoresist, this produces a slope in the ramp of about 20° [47]. With a beam voltage of 500 V, the etching rate for the MgB_2 is about 8 nm min^{-1}. After removing the photoresist, a 12 nm MgO barrier layer was deposited by ablating Mg for 6 s at 10 Hz, in 0.5 mbar of oxygen at 200 °C. Subsequently, the deposition of 200 nm MgB_2 as a counter electrode was done similarly as for the base electrode, at 200 °C and at an Ar pressure of 0.17 mbar, followed by 5 min annealing at 600 °C. The sample is patterned by standard photolithography and ion milling to define the junctions, contact pads and the overlap of the counter electrode of 3 μm. The transition temperatures of both MgB_2 layers exceed 23 K.

Figure 3 displays the current–voltage (I–V) characteristics of a 7 μm wide junction at $T = 4.2$ K. These characteristics follow well the behaviour expected from a resistively shunted

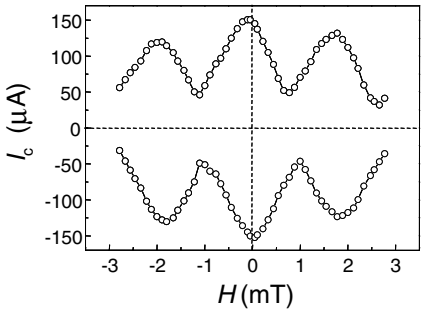

Figure 4. Modulation of the critical current of the junction of figure 3 as a function of the applied magnetic field H perpendicular to the current direction and parallel to the substrate (from [45]).

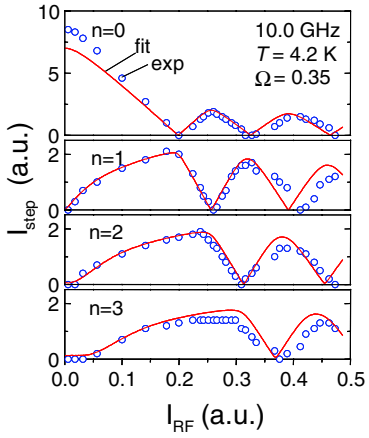

Figure 5. The amplitude of the supercurrent and the first three Shapiro steps versus applied RF current (10.0 GHz) at $T = 4.2$ K. The solid line shows a fit using the current-source model (from [45]).

junction (RSJ) model. At this temperature the critical current of this junction is 130 μA, which implies that the junction is in the small limit. The junction exhibits an excess current of about 30% of I_c at 4.2 K. The normal state resistance R_n is almost independent of temperature and has a value of about 1 Ω. The I_cR_n product at 4.2 K is 130 μV. Above 16 K, the critical current of the junction is suppressed completely by thermally activated phase slippage.

The application of a magnetic field H perpendicular to the current direction and parallel to the substrate resulted in a modulation of the critical current (figure 4). The critical current could be suppressed by up to 70%. The $I_c(H)$ dependence differs from the ideal Fraunhofer pattern that is expected for a small junction with a uniform current distribution. The large amplitude of the higher-order peaks and the incomplete suppression of the critical current are signatures of non-homogeneity of the barrier. This could be explained by the roughness of the ramp invoked by the surface roughness on the deposited film.

A complete suppression of the supercurrent and the formation of Shapiro steps at multiples of $V = 20.7$ μV were observed by irradiating the junction with 10.0 GHz microwave fields at 4.2 K (see inset, figure 3). The voltages at which the current steps appear are as expected from the frequency of the applied radiation ν_r:$V_n = (h/2e)\nu_r n$, with $2e/h = 483.6$ MHz μV^{-1}.

The modulation of the height of the Shapiro steps as a function of applied RF current is presented in figure 5. With

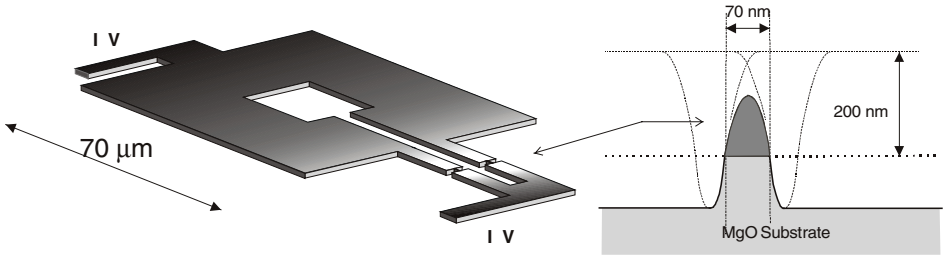

Figure 6. SQUID layout (left) and cross section of one of the nanobridges (right).

the RSJ model including the RF current-source term (for a description see, e.g., [48]), a good fit to the experimental data was obtained. It is noted that the fitting parameters were the same for all the Shapiro steps. The parameter Ω describing the ratio of the RF and the critical frequency (proportional to I_cR_n) was found to be 0.35 from the fit, close to the expected value from the observed I_cR_n product under dc conditions.

In order to determine the effect of the interfaces between the MgO barrier and the electrodes on the junction transport properties, reference samples were prepared following the same fabrication procedure, except for the deposition of the barrier layer. It has been shown, e.g., in high-T_c Josephson junction technology [49], that a barrier can be formed by the interface between the electrodes due to structural damage invoked by the ion milling. In contrast, for the MgB_2 ramp type contacts, this ion-milling procedure did not lead to weak link behaviour. Critical currents up to 31 mA were obtained for 5 μm wide contacts at 4.2 K, which corresponds to a critical current density of 3×10^6 A cm^{-2}. This implies that the interface region has good superconducting properties and will not affect the transport properties of the Josephson junctions. Furthermore, it indicates that the ramp type contact presents a good configuration for via contacts in future multilayer circuits.

From the above, it is concluded that the 12 nm MgO barrier forms the weak link in our Josephson junction. The non-hysteretic character of the I–V curve results from the low normal state resistance and the low value of the capacitance. The reduction of the I_cR_n product as compared to theoretical predictions [8] may arise from the non-homogeneities in the barrier. It is consistent with the observation of excess current in the I–V characteristics and the incomplete suppression of the critical current with applied magnetic field.

3.2. Fabrication of MgB_2 SQUIDs

The next step is the realization of SQUIDs. The procedures used so far for this are not foreseen to be suited for the realization of trilayer Josephson junctions because of the post-anneal step involved, except for the procedure as described above for ramp-type junctions. Fortunately, aside from Josephson junctions that include a barrier layer, nanobridges can also be employed as the weak links in a SQUID [50].

For the fabrication of the SQUIDs, first, thin films of 200 nm MgB_2 were deposited on MgO substrates by pulsed laser ablation in a two-step *in situ* process [20]. These films are polycrystalline, but this does not hamper the supercurrent since the grain boundaries in MgB_2 act as strong links.

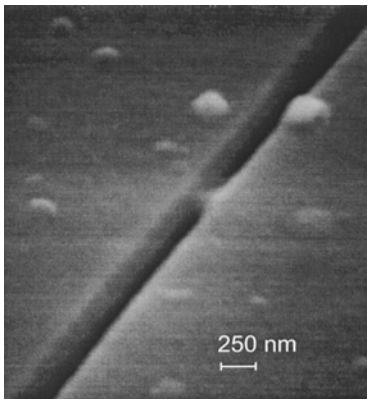

Figure 7. Scanning electron microscope image of a MgB_2 nanobridge.

The SQUID, with an estimated inductance of 60 pH consists of a square washer of 20×20 μm^2 inner and 70×70 μm^2 outer dimensions, and a 5×55 μm^2 slit as shown in figure 6. Further, the structure contains two striplines 30 μm long and 5 μm wide into which, subsequently, nanobridges (70×150 nm^2) were structured by direct FIB milling, see figure 7.

The transition temperature of the structure was found to be 22 K, comparable to the original T_c value of the unpatterned film. In figure 8, a typical example of the measured SQUID I–V characteristics is shown for the two external values of the enclosed magnetic flux of the SQUID at a temperature $T = 19$ K. Above $T = 12$ K, the I–V characteristics are non-hysteretic, with a parabolic shape of the voltage branch; below 12 K hysteresis appears, most likely because of the heating of the nanobridge. At temperatures below 10 K, large bias currents are needed to suppress the superconducting properties of the nanobridge. An example of this hysteresis is given for a junction at 10 K in the inset of figure 8. The kinks in the voltage branch are an indication of the onset of additional channels for vortex flow [51].

The critical current of the SQUID at $T = 4.2$ K is 1.5 mA. With an estimated bridge cross section of 70×150 nm^2 this results in a critical current density of 7×10^6 A cm^{-2}. This large value implies that the nanostructuring by the use of a Ga focused ion beam is very well possible while maintaining large critical current densities. This is important information since it shows that the chemical reactivity and volatility of magnesium do not pose problems in the nanostructuring. Furthermore, the structures are very stable over time and insensitive to thermal cycling or exposure to moisture.

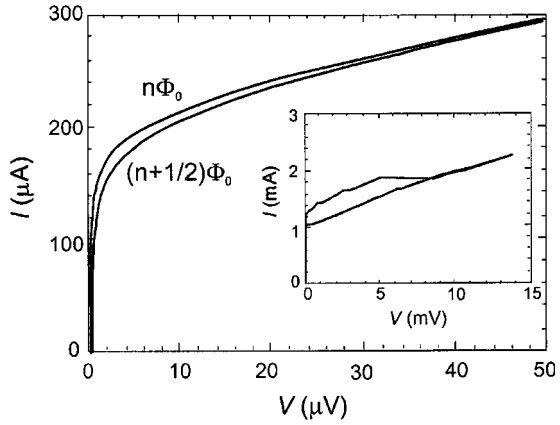

Figure 8. I–V characteristics of a MgB_2 SQUID at $T = 19$ K for different values of the enclosed magnetic flux. The inset shows a typical example of the hysteresis of the junctions below 12 K. The data are obtained at 10 K (from [37]).

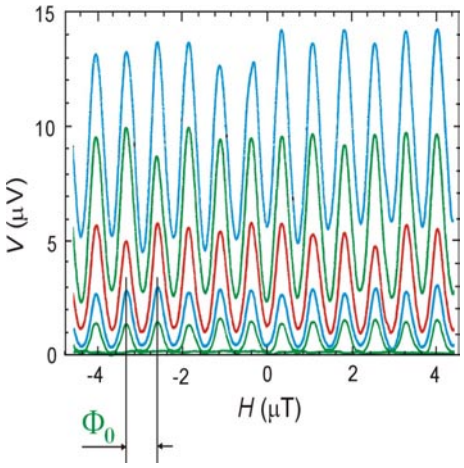

Figure 9. SQUID voltage modulation at 15 K at different values of the current bias. The period of oscillation corresponds to 1 Φ_0 (from [37]).

In figure 9, the voltage modulation of the SQUID at different constant bias currents is shown as a function of the applied magnetic field. The period of the modulation is 0.74 μT. With a period of Φ_0 for the SQUID critical current modulation by applied magnetic flux, an effective SQUID area $A_{\rm eff} = \Phi_0/H$ of 2.8×10^3 μm^2 is obtained, which is in good accord with the actual SQUID dimensions, taking flux focusing by the superconducting washer into account. Above the temperature at which the I–V characteristics become hysteretic, the voltage modulation shows the same temperature dependence as the critical current. A modulation voltage of 30 μV was observed at 10 K.

4. Conclusions

The results presented on ramp-type Josephson junctions as well as SQUIDs made from nanobridges prove that high-quality superconducting structures can be realized on a length scale <100 nm in *in situ* fabricated MgB_2 films. An important issue is the noise behaviour of the junctions and SQUIDs. If progress can be made in the fabrication of high quality (epitaxial) thin films with T_c approaching the bulk value of 39 K and noise properties that are better than (or comparable with) the oxide superconductors, MgB_2 will find its application in the field of sensors and electronic circuits.

Acknowledgments

The authors acknowledge the contributions of A A Golubov, G J Gerritsma, H M Christen, C-B Eom, R H Hammond, D C Larbalestier, J M Rowell, D Schlom and X X Xi in helpful discussions and sharing information.

This work was supported by the Dutch Foundation for Research on Matter (FOM) and the strategic orientation Materials Science of Interfaces of MESA$^+$ Research Institute, University of Twente.

References

[1] Nagamatsu J, Nakava N, Muranaka T, Zenitani Y and Akimitsu J 2001 *Nature* **410** 63
See also, Cava R J 2001 *Nature* **410** 23
[2] Bud'ko S L, Lapertot G, Petrovic C, Cunningham C E, Anderson N and Canfield P C 2001 *Phys. Rev. Lett.* **86** 1877
[3] Kortus J, Mazin I I, Belashchenko K D, Antropov V P and Boyer L L 2001 *Phys. Rev. Lett.* **86** 4656
[4] An J M and Pickett W E 2001 *Phys. Rev. Lett.* **86** 4366
[5] Kong Y, Dolgov O V, Jespen O and Anderson O K 2001 *Phys. Rev.* B **64** 020501
[6] Bohnen K P, Heid R and Renker B 2001 *Phys. Rev. Lett.* **86** 5771
[7] Liu A Y, Mazin I I and Kortus J 2001 *Phys. Rev. Lett.* **87** 087005
[8] Brinkman A *et al* 2002 *Phys. Rev.* B **65** 180517
[9] Golubov A A *et al* 2002 *J. Phys.: Condens. Matter* **14** 1353
[10] Choi H J, Roundy D, Sun H, Cohen M L and Louie S G 2002 *Nature* **418** 758
[11] Golubov A A, Brinkman A, Dolgov O V, Kortus J and Jepsen O 2002 *Phys. Rev.* B **66** 054524
[12] Canfield P C *et al* 2001 *Phys. Rev. Lett.* **86** 2423
[13] Larbalestier D C *et al* 2001 *Nature* **410** 186
[14] Kambara M *et al* 2001 *Supercond. Sci. Technol.* **14** L5–7
[15] Finnemore D K, Ostenson J E, Bud'ko S L, Lapertot G and Canfield P C 2001 *Phys. Rev. Lett.* **86** 2420
[16] Kang W N, Kim H J, Choi E M, Jung C U and Lee S I 2001 *Science* **292** 1521
[17] Bu S D *et al* 2002 *Appl. Phys. Lett.* **81** 1851
[18] Hur N *et al* 2001 *Appl. Phys. Lett.* **79** 4180
[19] Eom C B *et al* 2001 *Nature* **411** 558
[20] Brinkman A *et al* 2001 *Physica* C **353** 1
[21] Blank D H A, Hilgenkamp H, Brinkman A, Mijatovic D, Rijnders G and Rogalla H 2001 *Appl. Phys. Lett.* **79** 394
[22] Shinde S R *et al* 2001 *Appl. Phys. Lett.* **79** 227
[23] Christen H M *et al* 2001 *Physica* C **353** 157
[24] Ermolov S N *et al* 2001 *JETP Lett.* **73** 557
[25] Mijatovic D, Brinkman A, Rijnders G, Hilgenkamp H, Rogalla H and Blank D H A 2002 *Physica* C **372–6** 1258
[26] Saito A, Kwakami A, Shimakage H and Wang Z 2002 *Japan. J. Appl. Phys.* **41** L127
[27] Ueda K and Naito M 2001 *Appl. Phys. Lett.* **79** 2046
[28] Jo W, Huh J U, Ohnishi T, Marshall A F, Beasley M R and Hammond R H 2002 *Appl. Phys. Lett.* **80** 3563
[29] Zeng X H *et al* 2001 *Appl. Phys. Lett.* **79** 1840
[30] Kang W N, Choi E M, Kim H J, Kim H J and Lee S I 2002 *Preprint* cond-mat/0209226
[31] Amoruso S, Bruzzese R, Spinelli N, Velotta R, Wang X and Ferdeghini C 2002 *Appl. Phys. Lett.* **80** 4315
[32] Xi X X *et al* 2002 *Supercond. Sci. Technol.* **15** 451

[33] For more details, see Naito M, Sato H and Yamamoto H 1997 *Physica* C **293** 36
Naito M, Yamamoto H and Sato H 1998 *Physica* C **305** 233
[34] Mijatovic D, Brinkman A, Oomen I, Rijnders G, Hilgenkamp H, Rogalla H and Blank D H A 2002 MgB_2 thin films and Josephson devices *Proc. ASC*
[35] He T, Cava R J and Rowell J M 2002 *Appl. Phys. Lett.* **80** 291
[36] Zhai H Y, Christen H M, Cantoni C, Goyal A and Lowndes D H 2002 *Appl. Phys. Lett.* **80** 1963
[37] Brinkman A, Veldhuis D, Mijatovic D, Rijnders G, Blank D H A, Hilgenkamp H and Rogalla H 2001 *Appl. Phys. Lett.* **79** 2420
[38] Burnell G, Kang D J, Lee H N, Moon S H, Oh B and Blamire M G 2001 *Appl. Phys. Lett.* **79** 3464
[39] Burnell G *et al* 2002 *Appl. Phys. Lett.* **81** 102
[40] Zhang Y, Kinion D, Chen J, Hinks D G, Crabtree G W and Clark J 2001 *Appl. Phys. Lett.* **79** 3995
[41] Gonnelli R S, Calzolari A, Daghero D, Ummarino G A and Stepanov V A 2001 *Phys. Rev. Lett.* **87** 097001
[42] Carapella G, Martucciello N, Costabile G, Ferdeghini C, Ferrando V and Grassano G 2002 *Appl. Phys. Lett.* **80** 2949
[43] Badr M H, Fremat M, Sushko Y and Ng K W 2002 *Phys. Rev.* B **65** 184516
[44] Carapella G *et al* 2002 *Appl. Phys. Lett.* **80** 2949
[45] Mijatovic D *et al* 2002 *Appl. Phys. Lett.* **80** 2141
[46] Gao J, Aarnink W A M, Gerritsma G J and Rogalla H 1990 *Physica* C **171** 126
[47] Blank D H A and Rogalla H 1997 *J. Mater. Res.* **12** 2952
[48] See, e.g., Barone A and Paterno G 1982 *Physics and Application of the Josephson Effect* (New York: Wiley)
Likharev K K 1986 *Dynamics of Josephson Junctions and Circuits* (London: Gordon and Breach)
[49] Moeckly B H and Char K 1997 *Appl. Phys. Lett.* **71** 2526
[50] Pedyash M V, Blank D H A and Rogalla H 1996 *Appl. Phys. Lett.* **68** 1156
[51] de Nivelle H J M E, Gerritsma G J and Rogalla H 1993 *Phys. Rev. Lett.* **70** 1525